

Motion of the dusk flank boundary layer caused by solar wind pressure changes and the Kelvin-Helmholtz instability: 10–11 January 1997

D. H. Fairfield,¹ C. J. Farrugia,² T. Mukai,³ T. Nagai,⁴ and A. Fedorov⁵

Received 11 July 2003; revised 24 September 2003; accepted 14 October 2003; published 24 December 2003.

[1] During an interval of steady northward IMF on 10–11 January 1997, Geotail and Interball spacecraft data at $X = -5$ to $-15 R_E$ on the dusk flank reveal magnetopause boundary layer motions caused by both solar wind pressure discontinuities and the Kelvin-Helmholtz instability. Several large, sudden changes in solar wind density caused the magnetopause to move across both spacecraft. Relative timing of these crossings along with corresponding geosynchronous and ground magnetic field changes allow study of the propagation of pressure fronts in the magnetosheath and the associated wave propagation in the magnetosphere. The wave in the boundary layer propagates down the tail faster than the pressure front in the magnetosheath, producing boundary motion ahead of the magnetosheath front. This boundary layer wave can bulge out the magnetopause, causing a spacecraft in the magnetosheath to become immersed in the magnetosphere for as long as 2 or 3 min before the higher density magnetosheath plasma arrives and compresses the boundary. The tailward convecting magnetosheath pressure front moves more slowly near the magnetopause than it does further out in the magnetosheath, distorting the front and enhancing the likelihood that the boundary layer wave will outrun the magnetosheath front. Integrating the velocity perpendicular to the boundary shows that the boundary waves can have amplitudes of at least 1 or 2 R_e . During periods of steady solar wind pressure, waves with periods of several minutes are observed in a boundary layer that are consistent with excitation of the Kelvin-Helmholtz instability. Magnetograms from five ground magnetometer chains show both pulsations initiated by the pressure discontinuities and ongoing wave trains probably related to the KH instability. *INDEX*

TERMS: 2748 Magnetospheric Physics: Magnetotail boundary layers; 2724 Magnetospheric Physics: Magnetopause, cusp, and boundary layers; 2728 Magnetospheric Physics: Magnetosheath; 2752 Magnetospheric Physics: MHD waves and instabilities; 2784 Magnetospheric Physics: Solar wind/magnetosphere interactions; *KEYWORDS:* KH instability, dusk flank boundary, magnetopause motion, magnetopause waves, pressure discontinuity effects

Citation: Fairfield, D. H., C. J. Farrugia, T. Mukai, T. Nagai, and A. Fedorov, Motion of the dusk flank boundary layer caused by solar wind pressure changes and the Kelvin-Helmholtz instability: 10–11 January 1997, *J. Geophys. Res.*, 108(A12), 1460, doi:10.1029/2003JA010134, 2003.

1. Introduction

[2] The magnetopause and its adjacent boundary layer are of great importance in magnetospheric physics since mass, energy, and particles entering the magnetosphere must pass through this region. This outer magnetospheric boundary is

continually in motion due both to the variable shocked solar wind plasma impinging on this region and to local instabilities which excite surface waves (e.g., the Kelvin-Helmholtz instability). Whatever their cause, these motions in turn generate hydromagnetic waves that propagate to Earth and throughout the magnetosphere where they can excite resonances [e.g., *Southwood and Kivelson*, 1990; *Samson*, 1991].

[3] The external pressure changes impinging on the magnetopause can be produced either by changes in the ambient solar wind or by changes produced in the foreshock [*Fairfield et al.*, 1990]. *Kaufmann and Konradi* [1969] studied Explorer 12 data in the subsolar region and found an inordinate number of brief magnetopause crossings of few minutes duration which they argued were probably due to solar wind pressure changes. They proposed a model where a pressure change sweeps past the earth compressing

¹Laboratory for Extraterrestrial Physics, NASA Goddard Space Flight Center, Greenbelt, Maryland, USA.

²Space Science Center, University of New Hampshire, Durham, New Hampshire, USA.

³The Institute of Space and Astronautical Science, Sagamihara, Kanagawa, Japan.

⁴Earth and Planetary Sciences, Tokyo Institute of Technology, Tokyo, Japan.

⁵Centre d'Etude Spatiale des Rayonnements, Toulouse, France.

the magnetosphere and creating a magnetopause wave that propagates ahead of the front convecting tailward in the magnetosheath. Although this model has frequently been discussed [e.g., *Sibeck*, 1990], to our knowledge it has not been directly observed prior to the observations presented below. Different magnetopause normal directions on recurrent inbound versus outbound magnetopause crossings were first seen by *Ledley* [1971] and have often been taken as evidence for tailward propagating waves on the boundary. Such waves have often been attributed to the KH (Kelvin-Helmholtz) instability [e.g., *Aubry et al.*, 1971].

[4] Boundary motions due to magnetopause processes are closely connected to the question of plasma entry to the magnetosphere. When the IMF is southward, dayside reconnection is well accepted as the primary process that allows plasma to enter the magnetosphere. When the IMF is northward the situation is less clear; magnetosheath plasma is still observed on closed magnetosphere field lines of the boundary layer even though subsolar reconnection is not expected to occur. The boundary layer can be very thin near the subsolar point but is more typically at least several tenths of an R_E (Earth radius) thick near noon [e.g., *Paschmann et al.*, 1993] and 1 R_E or more on the flanks. Plasma entry on the magnetosphere flanks [*Fujimoto et al.*, 1996, 1998a, 1998b; *Fairfield et al.*, 2000] may even be responsible for an unusually dense plasma sheet seen under these northward IMF conditions [*Terasawa et al.*, 1997]. The plasma that enters the boundary layer experiences some heating [*Scopke et al.*, 1981; *Paschmann et al.*, 1993; *Le et al.*, 1996] and it resides on the same field lines as energetic magnetosphere plasma, although the two populations tend not to mix in velocity space [e.g., *Fujimoto et al.*, 1998b].

[5] There are several proposed mechanisms for this plasma entry that are particularly likely under northward IMF conditions. (1) Diffusive entry by a not-well-understood process [e.g., *Scopke et al.*, 1981; *Lotko and Sonnerup*, 1995; *Phan et al.*, 1997, and references therein] is one possibility. (2) High-latitude reconnection in both hemispheres may convert a magnetosheath field line into a closed magnetosphere field line containing magnetosheath plasma [*Song and Russell*, 1992; *Sandholt et al.*, 1999]. If such reconnection occurs in only one hemisphere an intermediate situation is created that complicates data interpretation. *Le et al.* [1994, 1996] interpret field-aligned flows in the frontside boundary layer as supporting this process. (3) Velocity shear can lead to waves in the boundary region produced by the KH instability. This shear can either be that between flowing magnetosheath plasma and the boundary layer or the boundary layer and the magnetosphere proper. Sheared magnetic field accompanying this velocity transitions may stabilize this process so instability is most likely at the equatorial magnetopause when a very northward IMF leads to a magnetosheath field that is aligned with a northward equatorial magnetosphere field. Alternatively, the boundary layer to magnetosphere transition may be unstable since magnetic shear is less likely at this internal boundary. The KH instability is generally thought not to lead to particle entry [e.g., *Fujimoto and Terasawa*, 1995] which is why *Scopke et al.* [1981] explained observed periodicities by diffusive particle entry followed by KH instability at the inner boundary. *Otto and Fairfield* [2000], however, conducted MHD simulations that

showed that KH instability at the magnetopause could twist up the magnetic field in plasma vortices in which reconnection could occur, thus allowing the particle entry observed by *Fairfield et al.* [2000]. *Farrugia et al.* [2000, 2001] also noted a billowy structure in the boundary layer plasma with hot plasma of magnetospheric origin winding around cold plasma of magnetosheath origin. Other case studies of boundary waves [e.g., *Chen et al.*, 1993; *Chen and Kivelson*, 1993; *Kivelson and Chen*, 1995; *Kokubun et al.*, 2000] are invariably associated with northward IMF. An additional event occurred on the well studied days of 10–11 January 1997 where *Laakso et al.* [1998] concluded that KH waves were observed in the LLBL. *Stenuit et al.* [2002], however, in studying the same event concluded that these were not KH waves.

[6] In this paper we will revisit the 10–11 January 1997 interval where the IMF is unusually strong, steady, and northward while the plasma is dense, cool, and relatively steady except for several large abrupt kinetic pressure discontinuities. During this January interval the Geotail and Interball spacecraft are near the dusk flank detecting boundary motions, while geosynchronous Goes 9 measurements and ground data permit observation of the magnetosphere effects nearer Earth. With this configuration we are able to study effects of both the sudden pressure changes and also those that may be caused by the KH instability. The coupling of the magnetosphere/LLBL waves to geomagnetic pulsations in the inner magnetosphere were monitored by five ground magnetometer chains. The several R_E separation of the spacecraft and the sudden boundary motions allow the study of propagating structures and the determination of the spatial scales of the magnetopause/boundary layer. In particular, during large kinetic pressure variations, we shall advance evidence in favor of the Kaufmann and Konradi conceptual model of magnetopause distortions.

2. Solar Wind Conditions on 10–11 January 1997

[7] The 10–11 January 1997 interval has been the subject of a special issue (*Geophysical Research Letters*, 25(14), 1998) and a number of other papers, many concentrating on the moderate magnetic storm associated with a magnetic cloud whose trailing portion containing a strongly northward field that terminates near 0500 on 11 January [*Burlaga et al.*, 1998; *Farrugia et al.*, 1998, 2000]. This cloud contains the coolest solar wind electrons ever observed near Earth [*Larson et al.*, 2000], and these authors found evidence for thermal equilibrium of ions and electrons ($T_i = T_e$), which they attributed to the more frequent Coulomb collisions due to the low proton temperatures and the high densities. Solar wind data for the interval of interest here (10 January 2000 UT through 11 January 0800 UT) are shown in Figure 1 where the Wind measurements have been advanced by 23 min to account for the propagation time to Earth from the Wind location (94, -57 , $-5 R_E$). The Wind SWE proton measurements [*Ogilvie et al.*, 1995] shown in red may differ slightly from earlier presentations as the SWE experimenters have carefully reanalyzed the data in view of the very cool temperatures. Wind/MFI [*Lepping et al.*, 1995] magnetic field measurements are shown in black and IMP 8 measurements in blue. The Wind measurements usually agree closely with Imp

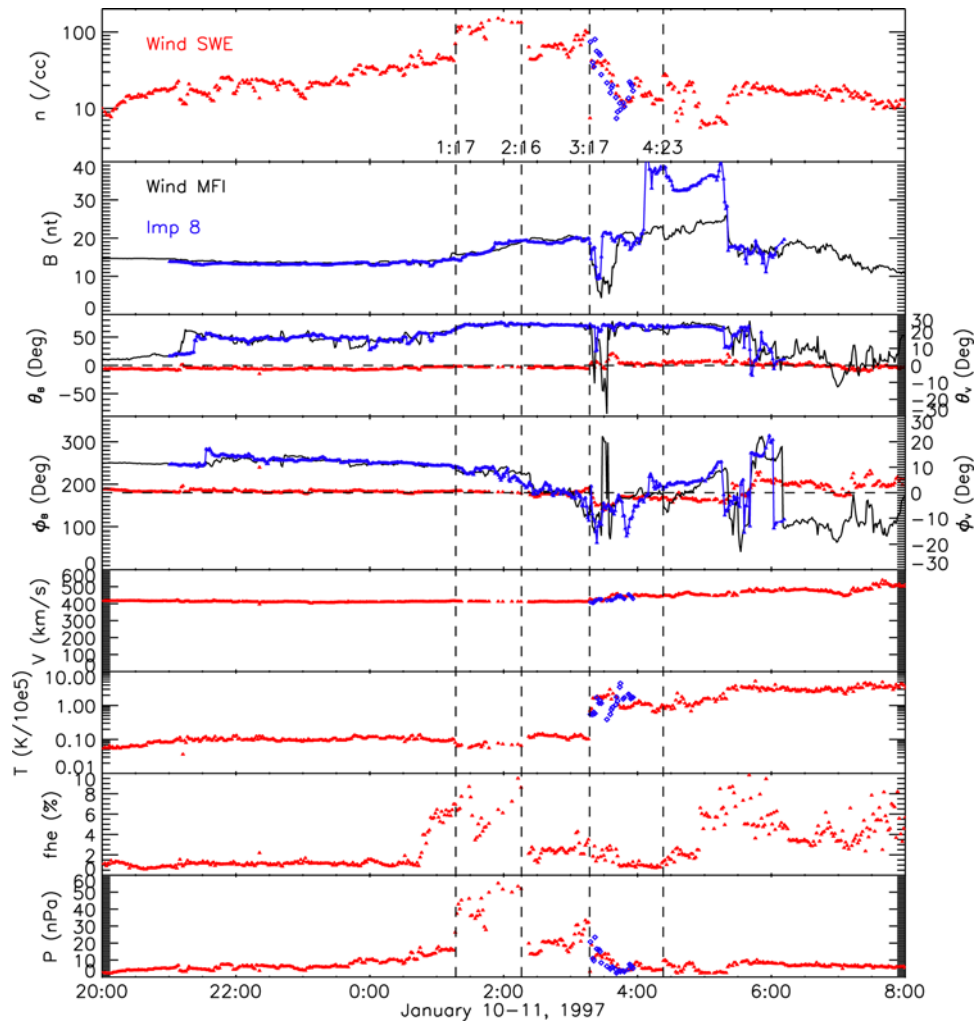


Figure 1. Solar wind measurements on 10–11 January 1997. Wind SWE proton measurements are shown in red and Wind MFI magnetic field measurements in solar ecliptic coordinates are in black. Imp 8 measurements are shown in blue. The large pressure discontinuities of interest here are indicated by vertical dashed lines. All measurements have been advanced by 23 min to account for the propagation time to Earth.

8 except for the enhanced Imp 8 field magnitude that occurs between 0405 and 0515 when this spacecraft is in the magnetosheath at solar magnetospheric location $(-8.5, 27.5, 24.5 \text{ Re})$. Note that the solar wind density reached unusually high values of over 150/cc in a pressure “plug” thought to contain prominence material [Burlaga *et al.*, 1998]. This plug created unusually high kinetic pressure above 50 nPa, which is about 25 times the average value for the solar wind. The features of particular interest here are the sudden increases or decreases in density at 0117, 0216, 0317, and 0423 that cause large variations in kinetic pressure incident on the magnetosphere.

[8] Figure 2 illustrates some of the magnetospheric effects of the abrupt solar wind pressure changes cited above. Figure 2a shows the horizontal component (H) of the Earth’s magnetic field measured by the geostationary Goes 9 spacecraft. At Goes 9, magnetic local time (MLT) is related to UT by $\text{MLT} = \text{UT} - 9$. The period shown thus refers to $\sim 1500\text{--}2100 \text{ MLT}$. Figure 2b repeats the Wind kinetic pressure from Figure 1. Figure 2c shows the

H component from the Japanese magnetometer station Chichijima at 20.6° magnetic latitude. The station is sweeping through the dayside, from MLT $\sim 0800\text{--}1400 \text{ MLT}$. This being a low-latitude station, it responds primarily to the ring current and the magnetopause current. During this time of northward IMF, the ring current was not enhanced, so the changes in magnetic field should be due primarily to the magnetopause currents or, equivalently, to compression by the enhanced solar wind plasma. These currents are proportional to the square root of the solar wind dynamic pressure [e.g., Russell *et al.*, 1992, and references therein] and they are shown by the thin trace in Figure 2c. The proportionality constant is estimated as $10.5 \text{ nT}/(\text{nPa})^{-1/2}$ [Russell *et al.*, 1992; Freeman and Farrugia, 1998, and references therein] with the internal currents adding an additional 50% [Chapman and Bartels, 1940]. A proportionality constant of $15.5 \text{ nT}/(\text{nPa})^{-1/2}$ has been used in calculating the currents in Figure 2c. Clearly, there is good agreement between the measured and the predicted disturbances from this source.

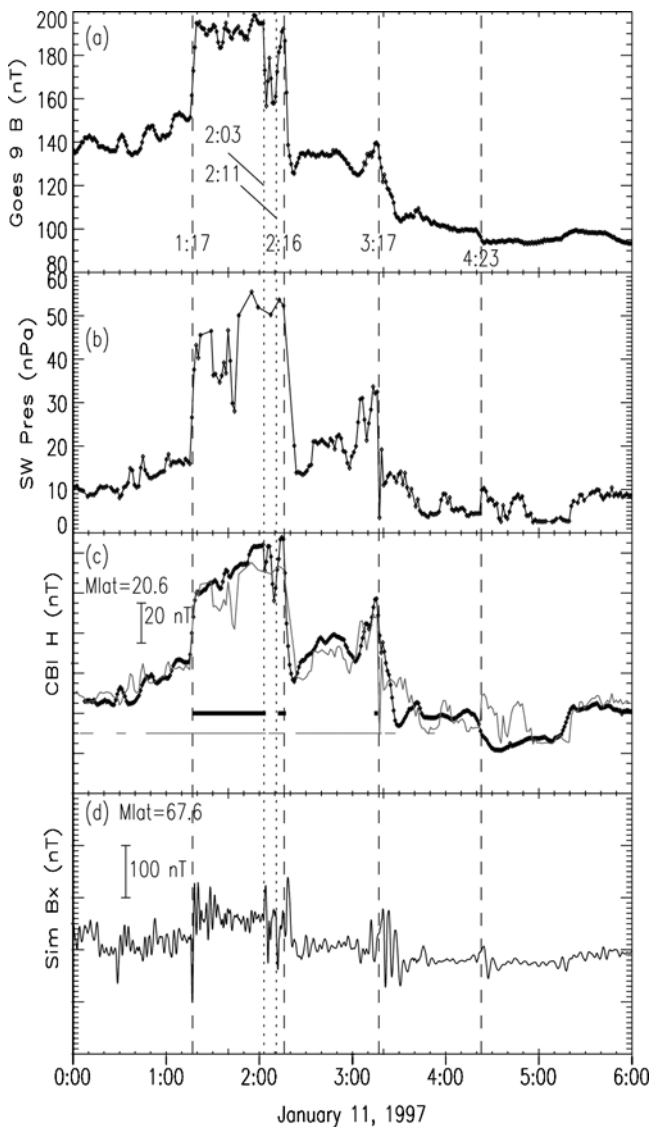


Figure 2. Magnetosphere observations with solar wind pressure. (a) Magnetic field strength measured by Goes 9. (b) The solar wind kinetic pressure measured by Wind SWE and advanced 23 min. (c) The magnetic field H component from the ground station Chichijima (heavy trace) and the effects of magnetopause currents calculated from the solar wind pressure (thin trace). (d) The magnetic field X component from the auroral zone station Fort Simpson. Horizontal bars in Figure 2c indicate periods when Geotail (thin trace) and Interball (thick trace) spacecraft were located in the magnetosheath. Vertical dashed lines indicate the solar wind pressure changes and vertical dotted lines indicate inferred pressure changes not clearly seen by Wind.

[9] Figure 2d shows the B_x component of the Canopus magnetometer chain station Fort Simpson at 67.6° magnetic latitude. This station covers the MLT range ~ 1500 – 2100 MLT during the interval. (See Figure 10 in the work of *Farrugia et al.* [2000] for data from the complete chain of stations.) The sensitivity scales in Figure 2a and 2c are virtually the same whereas the high-latitude station in Figure 2d is a factor of 5 less sensitive. In addition to

observing the effects of magnetopause currents associated with compression, large-amplitude oscillations are observed that will be discussed in more detail below. Here we note that in every clear case, the initial pulse of the high latitude perturbation in Figure 2d is opposite to the sense of the pressure change. This is a known effect at this high-latitude duskside local time [*Tamao*, 1964; *Nishida*, 1978].

[10] A simple calculation of the propagation time of the solar wind from Wind to Earth using the X separation is $94R_E/410 \text{ km/s} = 24 \text{ min}$ but this value could have several minutes uncertainty. In this figure and Figure 1 we have added 23 min to align the measured Wind pressure with the ground data. Intervals when Geotail and Interball (both of which were on the dusk flank of the magnetosphere) were in the magnetosheath (as discussed later) are marked with horizontal thin and thick black bars respectively in Figure 2c. These magnetosheath times have been moved backward in time by 4 min to align them with the ground changes showing that the effects of the solar wind at geostationary orbit and the ground precede those at the flank magnetosphere. These entries and exits from the magnetosheath generally correspond to increases and decreases in the kinetic pressure and magnetometer traces and will be discussed in more detail below.

[11] A prime motivation for Figure 2 is to point out that the changes in all three magnetometer traces at 0203 UT (a dotted vertical line) associated with the entry of both Geotail and Interball into the magnetosphere suggest a solar wind plasma decrease that Wind failed to observe, either because of Wind's large Y separation from earth or because of the difficulty in making measurements of the very dense, cool, solar wind plasma present at this time (note the missing data points in solar wind pressure near this time which are due to difficulties analyzing the very dense cool plasmas). A reentry of Interball into the magnetosheath at 0211 (second dotted line) corresponds to increasing geomagnetic field, suggesting that the solar wind pressure increased again before the final solar wind decrease that was observed by Wind at 0216.

3. Spacecraft Locations

[12] The XY and XZ orbital plots of Interball and Geotail in solar magnetospheric coordinates are shown in Figure 3a and 3b, respectively, with the hours of 10–11 January indicated on the trajectory segments. The heavy lines in Figure 3a illustrate the *Shue et al.* [1998] magnetopause calculated for two extremes of pressure from the period of interest. The perpendicular distances of Geotail and Interball from the Shue et al. model magnetopause as a function of time are shown in Figure 3c. Input to the model is the Wind SWE proton and helium density, velocity, and the Wind MFI magnetic field B_z component. The effects of nonradial solar wind flows were also removed using the SWE measured flow direction. Predicted locations outside the magnetopause are positive and inside are negative. The thinner and thicker black bars in Figure 3c indicating residence of Geotail (thinner) and Interball (thicker) in the magnetosheath are repeated from Figure 2c. Clearly, the model predictions are rather good; Interball is predicted and observed to be outside the magnetopause during the high-density pulse and Geotail is outside whenever it is predicted

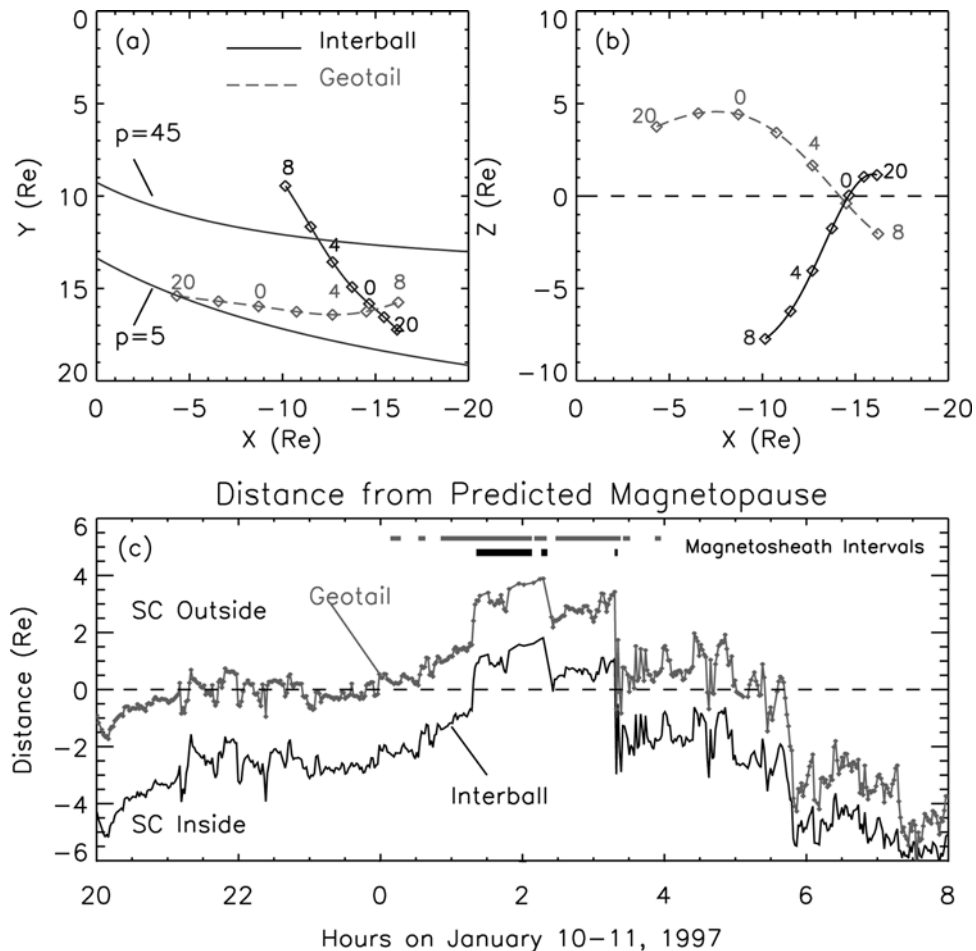


Figure 3. Showing spacecraft location relative to the magnetopause. (a) XY projections of Geotail and Interball trajectories in relation to two locations of the magnetopause corresponding to two extremes of the solar wind pressure. (b) XZ projections of the trajectory. (c) Distance of the spacecraft from the *Shue et al.* [1998] model magnetopause as a function of time.

to be. There are, however, numerous intervals when Geotail is predicted to be as much as $1 R_E$ outside when it was actually within the boundary layer. Figure 4 compares the time-shifted, more steady solar wind density and velocity with the simultaneous, highly variable measurements from Geotail. Intervals when Geotail is in the magnetosheath can be recognized from their densities greater than the solar wind along with less variable velocities slightly less than the solar wind. Clearly, the interval before 0008 is not magnetosheath, suggesting that the model boundary should be at least $0.5 R_E$ further out. (Note that this 11 January interval was used by *Shue et al.* [1998] in evaluating their improved magnetopause model, but these authors identified most of the Geotail interval between 0020 and 0540 as magnetosheath whereas we would argue that much of it is boundary layer.)

4. Solar Wind Density Increases Observed in the Magnetosheath

[13] To understand the observations of a sudden solar wind pressure change when observed in the magnetosheath and on the ground, it is useful to review the expectations

from theory. *Völk and Auer* [1974] and *Wu et al.* [1993] determined how a tangential discontinuity associated with a solar wind density discontinuity interacts with the bow shock. These authors found that additional features appear as a pressure discontinuity moves through the bow shock; the bow shock moves earthward and a fast mode wave is produced that propagates ahead of the pressure discontinuity. In effect, a solar wind pressure increase in the magnetosheath is distributed over two discontinuities. Although this theoretical work is basically a local analysis near the bow shock, it is clear that in actuality the fast mode wave will travel to the magnetopause where it will initiate magnetosphere compression. One wave will propagate back to the bow shock and thus begin slowing earthward motion of the shock in a complicated process of successive reflections that will result in the shock reaching a new equilibrium position. Another compressional wave in the magnetosphere will propagate earthward and tailward inside the magnetopause.

[14] It was realized many years ago [*Kaufmann and Konradi*, 1969; *Sibeck*, 1990] that due to the high fast mode wave velocity in the magnetosphere, this compressional wave would rapidly reach Earth and also propagate tailward inside the magnetopause with a velocity slower than that

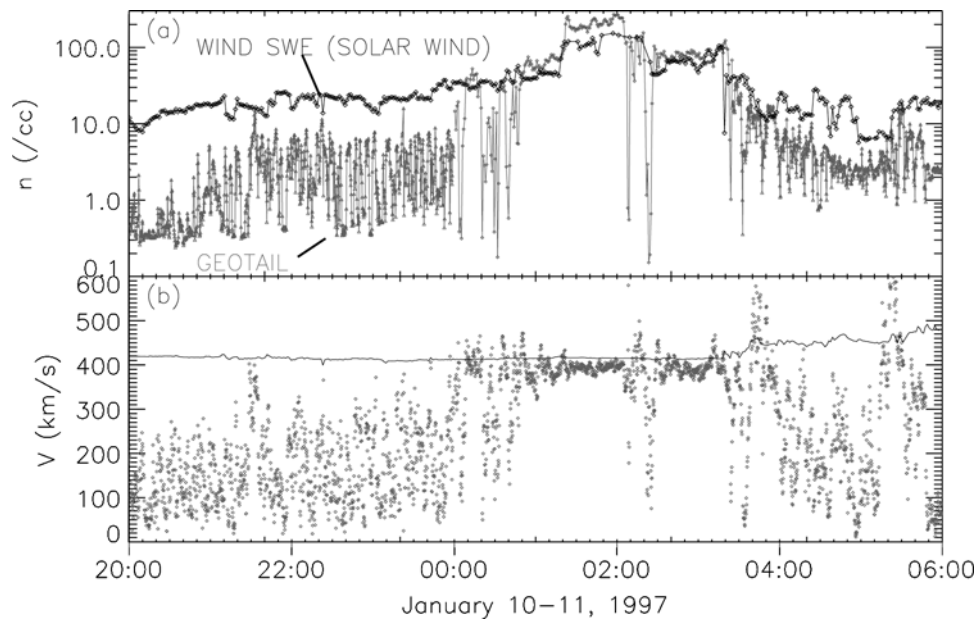


Figure 4. Time shifted solar wind density (a) and velocity (b) are compared to the same quantities measured by Geotail. Intervals where Geotail densities exceed solar wind densities and Geotail velocities are near the solar wind velocity together indicate Geotail residence in the magnetosheath. Prior to 0008 Geotail resides within the boundary layer.

propagating to Earth but which typically would be larger than the plasma velocity carrying the magnetosheath pressure discontinuity front tailward. Such a magnetopause wave would bulge out the magnetopause into the lower pressure magnetosheath ahead of the increase and cause a weakened magnetosphere field in its trailing portion to conserve magnetic flux. This theoretical idea has been extensively discussed by *Sibeck* [1990] although we are not aware of any direct observations of this phenomena on the flanks of the magnetosphere.

[15] We now study the above mechanism with data from 11 January 1997, including observations inside as well as outside the magnetospheric cavity. Just prior to the arrival of the first very large solar wind density enhancement in the dusk magnetosheath at 0117, Geotail is predicted to be about $1.5 R_E$ outside the magnetopause and Interball $1 R_E$ inside the magnetopause as can be seen in Figure 3c. Geotail at solar magnetospheric location $(-10.10, 16.15, 3.84 R_E)$ is about $4 R_E$ sunward of Interball $(-14.04, 15.25, -1.10 R_E)$. Figure 5 presents data from these spacecraft. Figure 5a shows an electron spectrogram from the Interball ELECTRON experiment from the detector facing sunward. Figure 5b shows the solar wind density in black and density from the Geotail CPI solar wind detector in red. Lacking accurate high-time-resolution density measurements from Interball, plasma flux from the Interball VDP instrument at 1 s resolution is shown in green with an arbitrary scale on the right. High-resolution Interball MIF (4 measurements per second) and Geotail MGF (16 measurements per second) are shown in Figures 5c and 5d. Magnetic field latitude angle θ is shown in 5e and Geotail velocity in 5f.

[16] The high Geotail densities and uniform flows confirm that Geotail remained in the magnetosheath throughout the interval of Figure 5 as predicted. The entry of Interball into the magnetosheath is marked by enhanced low-energy

fluxes in the spectrogram, an increase in Interball plasma flux, and a change of the Interball magnetic field to the northward magnetosheath orientation, all of which occur at 0121 20s (vertical green dotted line). The Geotail CPI instrument detects the solar wind density increase at 0121 46 (vertical dashed red line) where the more exact time of the increase is identified by the higher resolution LEP data (not shown because instrument saturation distorts the absolute values). This high-density arrival at Geotail is accompanied by a simultaneous decrease in the magnetosheath magnetic field (Figure 5d) from about 40 nT to 35 nT when averaged over the rapid ongoing mirror mode enhancements/rarefactions. (It is interesting to note that there is no change in the magnetic field direction at the time of this large density increase as can be seen from the constant θ value in Figure 5e and the constant φ angle shown in Figure 1. This fact means there is no normal field component and we can consider this as a tangential discontinuity in our subsequent comparison with theory.) With the magnetosheath velocity of 370 km/s measured by Geotail, a density discontinuity front aligned perpendicular to the magnetopause should take about 1 min to move from Geotail to Interball. In reality, however, Interball moved from the magnetosphere to the magnetosheath 25 s before the high density even arrived at Geotail further upstream. At 0124 15s Interball in the magnetosheath detected both a field decrease and plasma flux increase similar to that seen by Geotail 2.5 min earlier. The spectrogram suggests a cooling of the plasma that reflects the solar wind temperature decrease seen at this time in Figure 1. The highest flux saturates the Interball detector between 0124 15s and 0127, an interval of comparable length to the highest densities observed by Geotail 2.5 min earlier. We conclude that the two spacecraft are seeing the same magnetosheath structure, delayed by 2.5 min at Interball. If we assume the plasma

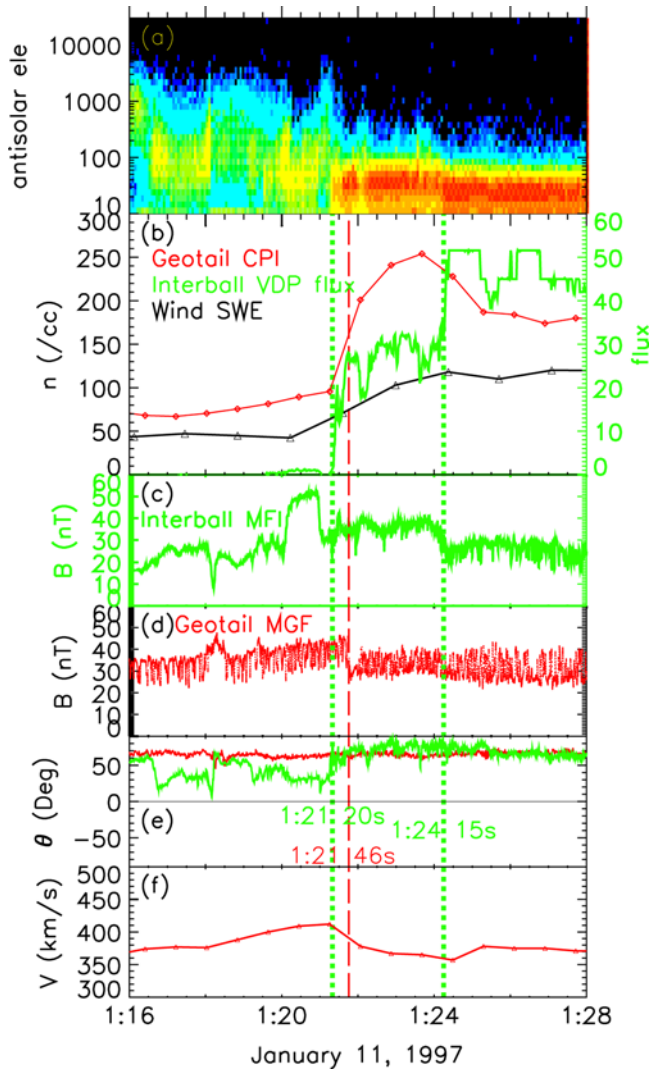


Figure 5. Measurements of the arrival of a pressure increase on the dusk flank. (a) An Interball electron spectrogram, (b) density measured by three spacecraft, (c) Interball magnetic field strength, (d) Geotail magnetic field strength, (e) Interball and Geotail north south θ angle, (f) Geotail velocity. Interball moves into the magnetosheath (vertical dotted line) before the pressure increase arrives at the upstream Geotail spacecraft (vertical dashed red line). The magnetosheath pressure increase subsequently arrives at Interball (vertical dashed green line).

encountering Geotail crossed the bow shock 2 min before the compressions were seen at GOES 9 and on the ground, the plasma would have traveled about $23 R_E$ in 6.8 min giving an average velocity of 360 km/s which is just below what was observed at Geotail.

[17] Figure 6a shows the spacecraft positions at 0122 rotated about the X axis into the XY plane. Dashed lines illustrate the magnetopause model for times before and after this 24 nPa pressure increase. The solid line illustrates the likely magnetopause position at the time Interball is exiting the magnetosphere as deduced by the following considerations. If the pressure front were aligned perpendicular to the magnetopause, the 2.5 min transit time from Geotail to

Interball and the spacecraft separation in X of $3.60 R_E$ (in a coordinate system aligned with the flow direction that flares at an angle of 14° to the X axis and is presumably parallel to the boundary) implies a transit velocity of 148 km/s which is very small compared with the observed Geotail plasma velocity of 370 km/s. This discrepancy can be explained by noting that flow on the streamline carrying the pressure front to Interball will pass nearer the subsolar point where the velocity is smaller, thus creating a longer delay time in

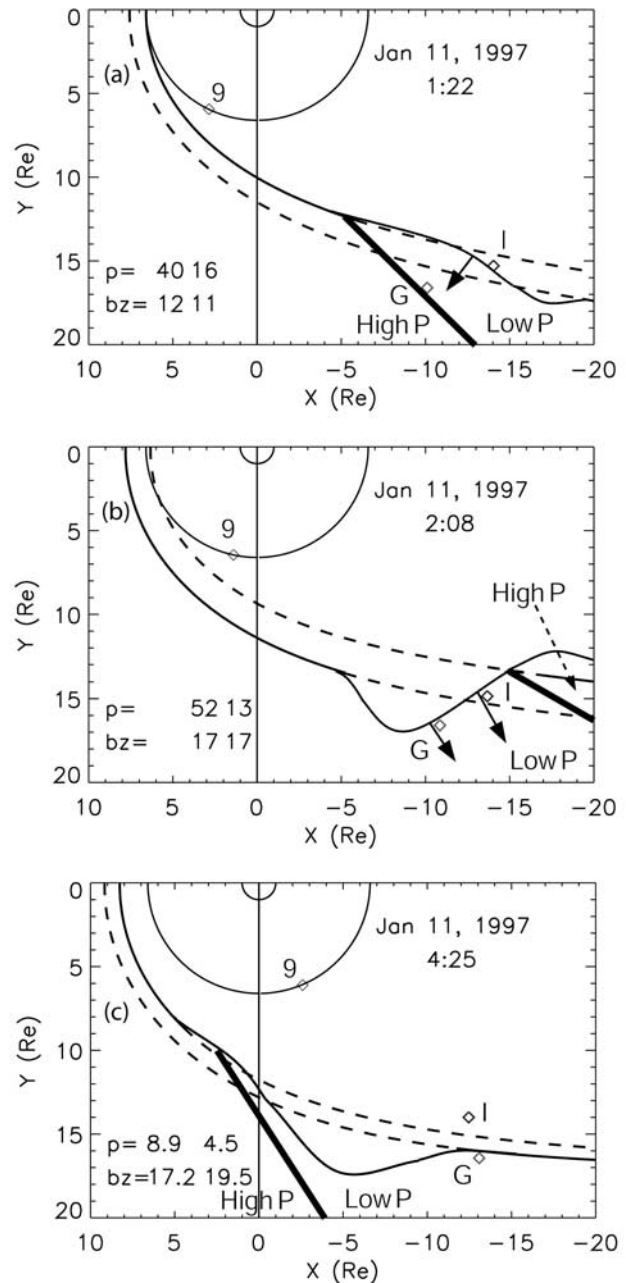


Figure 6. Deduced magnetopause positions (solid lines) for three periods when large pressure discontinuities were moving down the tail. Dashed lines represent the *Shue et al.* [1998] model magnetopause for times before and after the pressure change.

reaching Interball. At a velocity of 370 km/s the pressure front at Geotail will have been carried $5.1 R_E$ beyond the Interball position by the time the front intersects Interball (assuming that the velocity near the magnetopause has recovered to the higher value measured by Geotail). Given the $1.83 R_E$ Y spacecraft separation in the rotated frame, this implies that the front make an angle of 20° with magnetopause rather than the 90° it would have if the front were perpendicular to the magnetopause. The solid line separating the high and low density regions is drawn at this 20 degree angle such that it will encounter Geotail 25 s after the Interball exit, as is observed. The vector in Figure 6a is drawn in the magnetopause normal direction calculated from minimum variance on the Interball magnetic field. This direction further supports the picture as drawn.

[18] Although the applicability of the bow shock calculations of *Völk and Auer* [1974] and *Wu et al.* [1993] to the downstream magnetosheath is somewhat problematical, we note the following similarities between the 0121 event and the calculations and simulation of *Wu et al.* [1993]. The conditions of their Case A are rather similar to the observations. Their work shows that the primary density increase occurs at the tangential discontinuity which we would identify as 0121 46s in the Geotail data and 0124 15s at Interball in Figure 5 above. The simulation also shows that the density, velocity, and the magnetic field are all slightly enhanced between the leading fast mode wave front and the major pressure increase. Their fast mode wave propagates at a speed (in the Earth's reference frame) nearly equal to the upstream plasma flow velocity. At 400 km/s (nearly $4 R_E/\text{min}$) this wave probably travels some $30 R_E$ from the near-subsolar bow shock to the Geotail position which would take some 7 or 8 min and would arrive several minutes before the slower plasma. These few minutes is the time ahead of the major density increase that smaller Geotail enhancements were seen in density, velocity and magnetic field strength (0119–0121), all three of the parameters *Wu et al.* predict will increase. The fact that the simulation showed a sharp increase (fast mode shock) at the leading edge, whereas Geotail shows a more gradual increase, may be related to the additional reflected waves and the long elapsed time since shock formation at the bow shock. The simulation also shows a magnetic field strength on the trailing high-density side of the pressure front which is slightly lower than that on the low-density side. This can explain the decreased field strengths observed by both Geotail and Interball in the high-density region immediately following the density increases.

[19] The fact that Interball crosses the magnetopause into the magnetosheath before the major pressure pulse arrives at Geotail further upstream can be explained by a compressional wave inside the magnetopause boundary propagating ahead of the magnetosheath pressure front. The boundary would bulge outward into the lower pressure magnetosheath while a following magnetopause decompression can allow the boundary to move in as is illustrated in Figure 6a. Lacking Interball density we cannot compute the total magnetosphere pressure, but we note that the Interball magnetosphere magnetic field does approximately double from 0119 to 0121 before the boundary crossing. A Geotail close encounter with such a bulge might also be the explanation for the increase in the Geotail magnetosheath

field and the simultaneous brief cessation of mirror mode waves some 2 min earlier just after 0118. The higher magnetosheath pressure ahead of the major pressure increase would also help move the boundary inward. Note also that the compression at GOES 9 near the magnetopause began about 0116 or about 6 min before the exit of Interball from the magnetosphere some $20 R_E$ downstream. These numbers yield a propagation velocity of 350 km/s, but if the initial bulge arrived, say, 2 min before the exit, this propagation velocity in the magnetosphere would be more than 500 km/s which is indeed faster than the magnetosheath velocity measured by Geotail.

5. Magnetopause Encounters

5.1. The 0200–0230 Pressure Changes

[20] Sudden decreases as well as increases in the solar wind density also produce large and interesting movements of the magnetopause as are shown in Figure 7. The first significant solar wind decrease on 11 January reaches Geotail at about 0204 45s as indicated in Figure 7b by the red Geotail CPI density trace, with the exact time again determined from the saturated LEP data. This is the plasma decrease not seen in the Wind data but whose existence is inferred by the field decompression seen at GOES 9 and on the ground at 0203 UT in Figure 2. The ground/magnetosphere data suggest that this pressure decrease was followed by an increase some 8 min later and finally by the decrease that was observed by Wind (the dashed line at 0216 in Figure 2). This 0204 45s plasma decrease at Geotail corresponds to a decrease in B from 40 nT at 0204 45s to 25 nT at 2006 30 s as is shown in Figure 7d. The magnetic field then increased before the magnetopause was encountered at 0208 10s. The Interball magnetic field in Figure 7c shows a smaller decrease and the Interball plasma flux in Figure 7b show similar decrease to the Geotail density, both Interball decreases showing a 100 s delay relative to Geotail and reaching a minimum at 0207.

[21] There is also a decrease in total velocity at Geotail preceding entry to the magnetosphere as can be seen in the vectors in Figure 7f. This decrease may be due to the leading region of high-pressure expanding back sunward into the following low-pressure region for the following reasons. Within the ambient solar wind, there is pressure balance between the hotter, lower-density region and the cooler, higher-density region even though the higher-density region has much more kinetic energy in the Earth's frame. On passing through the bow shock where kinetic energy is converted to thermal energy, the higher-density region should have more thermal energy than the following lower-density region, creating a pressure imbalance in the magnetosheath. To rectify this imbalance, the leading high pressure will expand into the following lower-pressure region, thus decreasing velocity in the latter region. If we estimate that the plasma travels $30 R_E$ from the bow shock to Geotail at an average speed of 300 km/s, it will take 10.6 min to reach Geotail. If the magnetosheath Alfvén velocity (using estimated intermediate values of $n = 300$, $B = 40$, and $T = 5 \times 10^5$) is 50 km/s and the sound velocity is 83, giving a magnetosonic velocity of 97 km/s, the front will have time to expand almost $10 R_E$ sunward in the plasma frame of reference as the plasma convects to the spacecraft location.

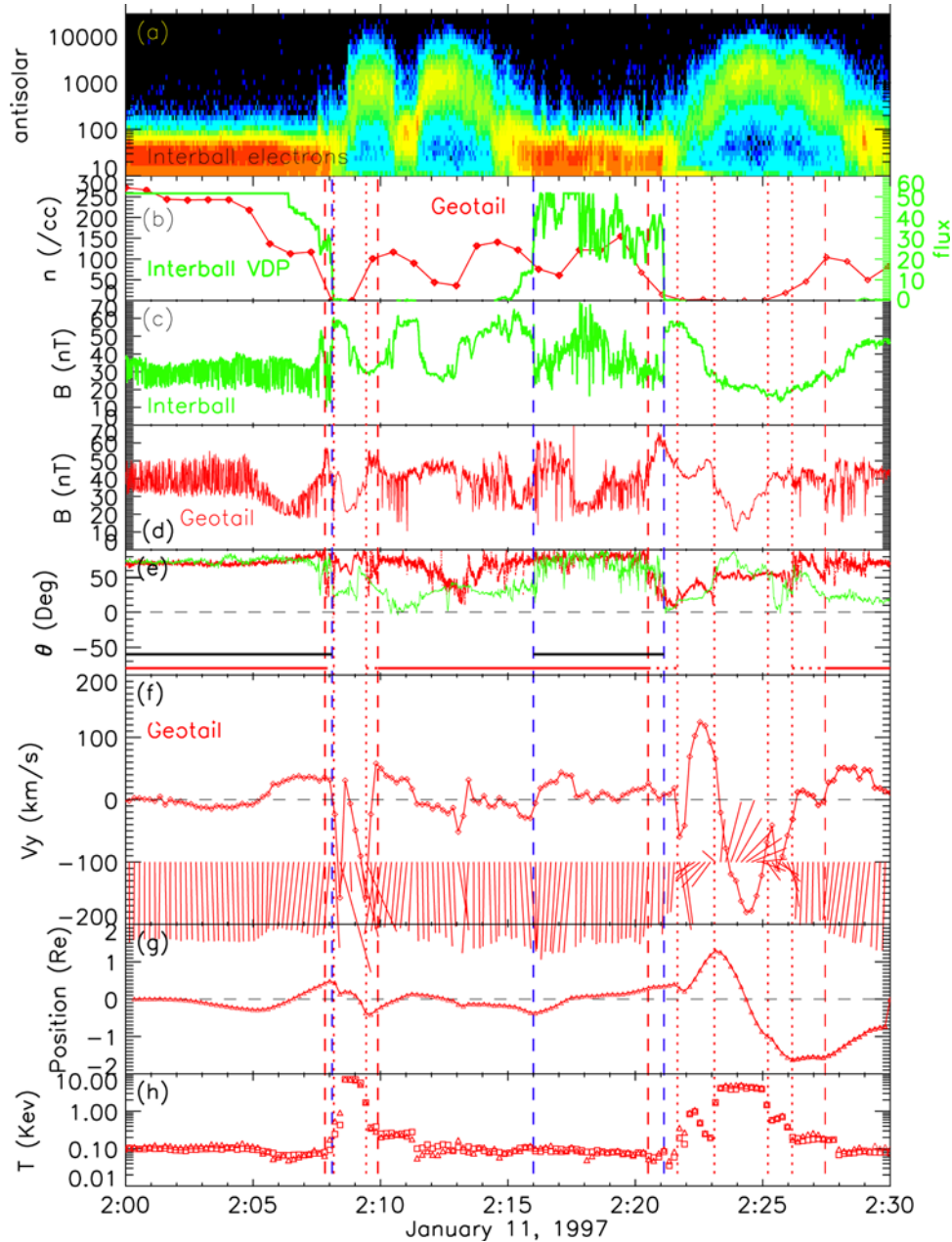


Figure 7. Interball and Geotail data in a format similar to Figure 5, with the addition of (f) the velocity trace V_y perpendicular to the magnetopause along with vectors (tailward V_x is downward and duskward V_y is toward the left), (g) the magnetopause motion obtained by integrating the V_y component, and (h) the ion temperature.

(The fast mode wave speed for propagation perpendicular to the field is $V_{ms} = (V_s^2 + V_A^2)^{1/2}$, where the sonic velocity $V_s = (\gamma p/\rho)^{1/2}$, with γ as the ratio of specific heats, p as the pressure, and ρ as the mass density, and the Alfvén velocity is $V_A = B/(4\pi\rho)^{1/2}$.) This expanded region would then take almost 3 min to convect back over Geotail which is the duration of the decreased velocity. This scenario may also explain the lowered Geotail density in the leading high-density region from 0202 to 0204. The decrease in B in the following low-density region seen by both spacecraft near 0206 is more difficult to explain. Ongoing KH waves apparently exist on the boundary before the density

decrease; *Farrugia et al.* [2000] noted a several minute period modulation of the Interball field strength which they attributed to boundary KH motion compressing the magnetosheath field. Perhaps the density decrease creates a second wave train of boundary motion that adds to the KH waves, with different phasing at the two spacecraft leading to the greater decrease at Geotail. The increase in B at 0207–0208 prior to entry to the magnetosphere is probably due to the outward expanding magnetopause compressing the adjacent magnetosheath field.

[22] Again we represent the boundary of the pressure front by a planar surface that moves from Geotail to Inter-

ball in 100 s at the magnetosheath velocity of 370 km/s. Using this timing and the spacecraft locations indicates that the front would make an angle of about 35° with the X axis as is drawn in Figure 6b. Interball entered the stable magnetosphere at 0208 6s, only a few seconds before the Geotail entry. A minimum variance analysis of the Geotail and Interball magnetic fields across the boundary yields boundary normal directions 12° and 8° , respectively, with the Y axis as is shown in Figure 6b. Clearly, these normals agree very well with the boundary orientation derived from timing the front arrival. The wavelength of the boundary is drawn to reflect the 76 s Geotail spends in the magnetosphere, assuming a magnetosheath-like velocity of 350 k/s. Geotail spends only 2.2 min in the boundary layer and magnetosphere before returning to the magnetosheath at 0209 58 s (vertical red dashed line). A subsequent minimum in Geotail density and θ angle near 0213 suggests another approach or entry to the boundary layer. This oscillatory behavior corresponds to similar fluctuations in the Interball magnetic field and the electron spectra in Figure 7a [see also *Farrugia et al.*, 2000] that is apparently associated with the decrease in GOES 9 and the CBI ground data 4 min earlier in Figure 2.

[23] The V_y velocity is shown by the red trace in Figure 7f. Actually, a rotation of approximately 15° has been performed so that this velocity is that perpendicular to a magnetopause flaring at this angle. This angle was determined by assuming the flow is parallel to the magnetopause and calculating a running average over a 10 min interval. Positive V_y is approximately duskward so the positive V_y from 0206 to 0208 is in the direction that would move a frozen-in boundary outward; indeed Geotail enters the magnetosphere during this period. Negative V_y after 0208 45s corresponds to a boundary moving inward and indeed the spacecraft returns to the magnetosheath after 0210. In Figure 7g, V_y has been integrated by summing the product of the 12 s sampling times and the measured V_y to give the distance of the motion. If we consider the region of variable field direction and intermediate temperature between the dashed and dotted lines as boundary layer, then this region is quite thin. If we consider the whole interval as boundary layer on the basis of its tailward flow (despite its high magnetosphere-like temperature), the layer is more like $0.3 R_E$ thick.

[24] Interball again joins Geotail in the magnetosheath at 0216 where it remains for 5 min (see vertical blue dashed lines). This crossing at 0216 is most probably due to the density increase beginning at 0211 as inferred from the magnetosphere/ground data in Figure 2. The subsequent rapid fourfold pressure decrease at 0216 in Figure 2 is undoubtedly the cause of both spacecraft entering the magnetosphere near 0221. During this entry, the density and field direction changes are more gradual at Geotail than at Interball, with the Geotail change spanning the interval 0220 30 to 0221 39. The higher-resolution LEP data not shown confirms the gradual decrease indicated by the CPI data. The red vertical Geotail entry line in Figure 7 has been placed at the beginning of the change (0220:30) which is 36 s ahead of Interball entry. This timing would require a boundary oriented almost perpendicular to the average boundary, but if the crossing were placed later, the picture would be similar to the 0208 crossing shown in Figure 6b. (Both Geotail and Interball measure negative B_x character-

istic of the southern magnetosphere despite the fact that Geotail's solar magnetospheric Z coordinate is positive 3 R_E . This apparent anomaly occurs because the dipole tilt angle is -29° at this time which will move the plasma sheet below the solar magnetospheric equatorial plane near midnight and raise it above this plane on the flanks. The lower magnetosphere field strength and greater θ angle at Geotail are consistent with a location nearer the effective equatorial plane.) Interball is 6 R_E south of Geotail and the former observes a more taillike field. After a slow outward motion prior to the 0221 crossing, the boundary region moves rapidly outward over Geotail as indicated by positive V_y velocities that reach as high as 100 km/s and persist for over 1 min. The velocities become negative near 0223 which moves the boundary downward returning Geotail to the magnetosheath at a time indicated as 0226 9s. The integrated velocity panel indicates inward and outward movement of more than 1 R_E . Note that the highest temperatures, which identify the magnetosphere proper, are associated with a region of sunward plasma flow.

5.2. Pressure Decrease at 0322

[25] A peak in the solar wind pressure, best indicated by the maxima at 0314 in Figure 2, is the likely cause of Interball briefly entering the magnetosheath for 2 min near 0319, the evidence being the intense low-energy electrons and the high Interball ion fluxes in Figure 8a and 8b. The Interball transitions to and from the magnetosheath provide a good illustration of the electrons gaining energy as they move from the magnetosheath to the boundary layer.

[26] A decrease in solar wind density from 100/cc to 40/cc at 0317 in Figure 1 is shown by the black trace in Figure 8b where the solar wind advance is 29 min as is appropriate for this downstream location. A magnetosheath B decrease begins at Geotail at 0318 30s and again the field increases before a boundary layer is entered at 0323. The magnetosheath velocity decreases in this region of depressed magnetosheath field outside the boundary, again suggestive of the leading high-density region expanding back upstream into the low-density region. Geotail remains in the LLBL/magnetosphere for only 2 min before returning to the magnetosheath. The V_y velocities are positive beginning near 0322, reflecting outward motion of the boundary that prevails until Geotail reaches the center of the magnetosphere interval where the velocities reverse. The integrated velocity (position) in Figure 8g suggests that the thickness of the boundary layer is again several tenths of a R_E with the spacecraft moving an additional distance into the magnetosphere proper. At this time the two spacecraft are at almost the same distance down the tail and the electron spectra indicate that Interball moved into the higher-temperature region at almost the same time although for a longer interval due to its location closer to the tail axis.

[27] Interpretation of this crossing is made difficult by the fact that the pressure decrease by more than a factor of two that moves the boundary outward is accompanied by a large 8 degree change in solar wind flow direction that moves the boundary in the opposite direction. This interval is also complicated by the fact that the IMF, rather than being steady and very northward as in all previous intervals, exhibits a brief sharp decrease before recovering to its very northward orientation. Figure 1 shows that the duration of

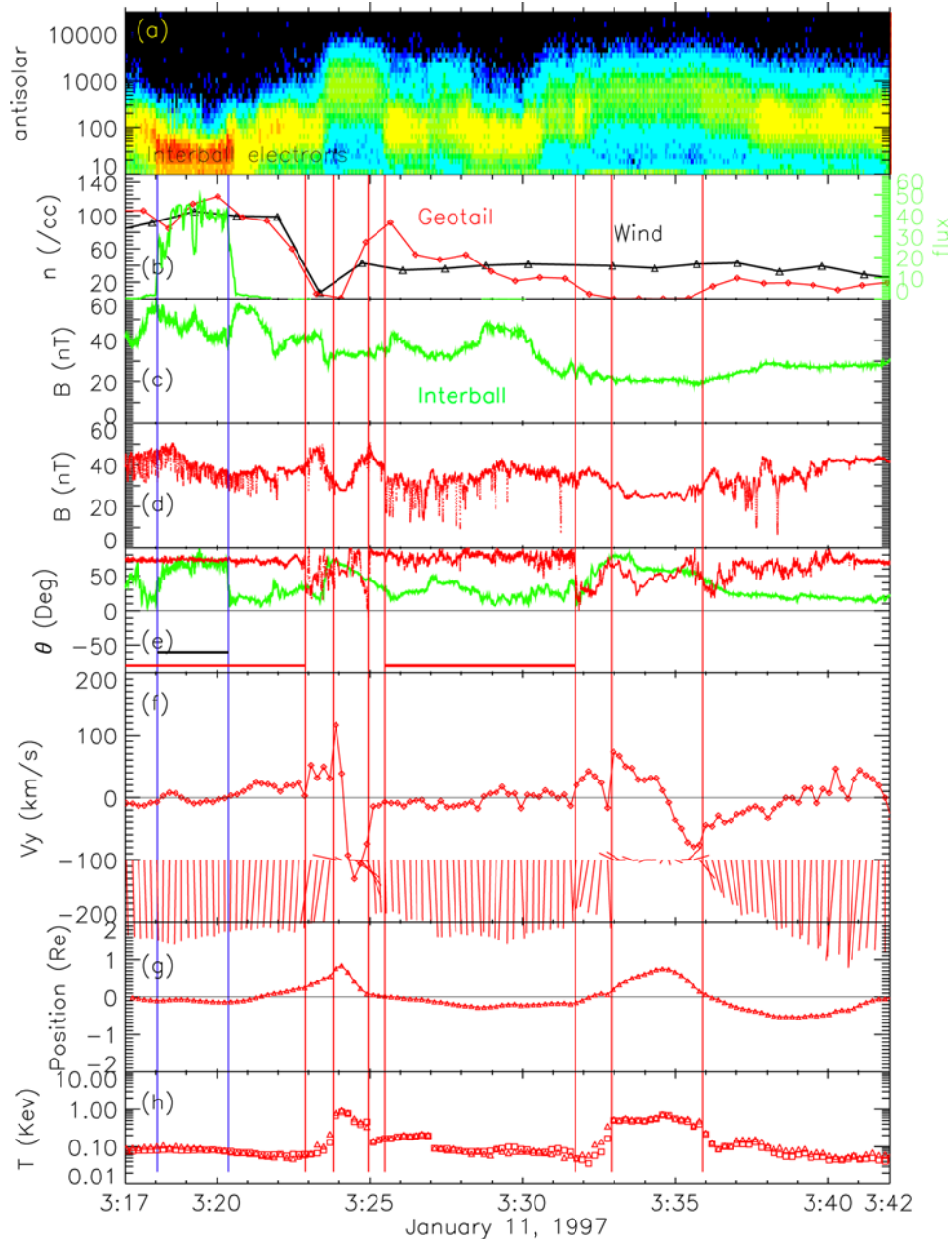


Figure 8. Interball and Geotail data in the same format as Figure 7.

this change is shorter at IMP 8 than Wind, reflecting spatial structure in the interplanetary medium.

5.3. Pressure Increase: 0425 UT

[28] During the interval 0420–0450 shown in Figure 9, Interball and Geotail both reside near $X = -13$ (see Figure 3) with Interball about $2 R_E$ closer to the tail axis and $6 R_E$ south of Geotail. The Interball VDP Instrument detects no ion flux and Geotail is mostly in the boundary layer as can be seen from the Geotail LEP densities in Figure 9d that are well below the solar wind density shown in blue. At 0425 Geotail begins to detect duskward moving plasma with velocities that persist for several minutes and become as high as 150 km/s (Figure 9f). This motion suggests a boundary layer of several R_E thickness outside the magnetosphere proper. (The center pair of vertical dashed lines in Figure 9 bracket a low-density,

high-temperature region that can be identified as the magnetosphere proper.) While Geotail V_y is positive, the φ angle of the Interball magnetic field gradually decreases from a value near 180° which, assuming a frozen in magnetic field, is consistent with the outward plasma motion measured by Geotail. The change in this field angle reverses sign near 0430 about a minute after the Geotail velocity reverses.

[29] This outward magnetosphere motion beginning at 0425 corresponds closely to a time when the solar wind pressure suddenly increases by a factor of 2 (See Figure 1 or the Wind density in Figure 9d where it has been advanced by 29 min as is appropriate to the downtail location). In fact, the outward motion begins about 3 min before this solar wind density increase reaches the Geotail position (assuming the 29 min advance). Although one might expect such a pressure increase would leave Geotail further out in the

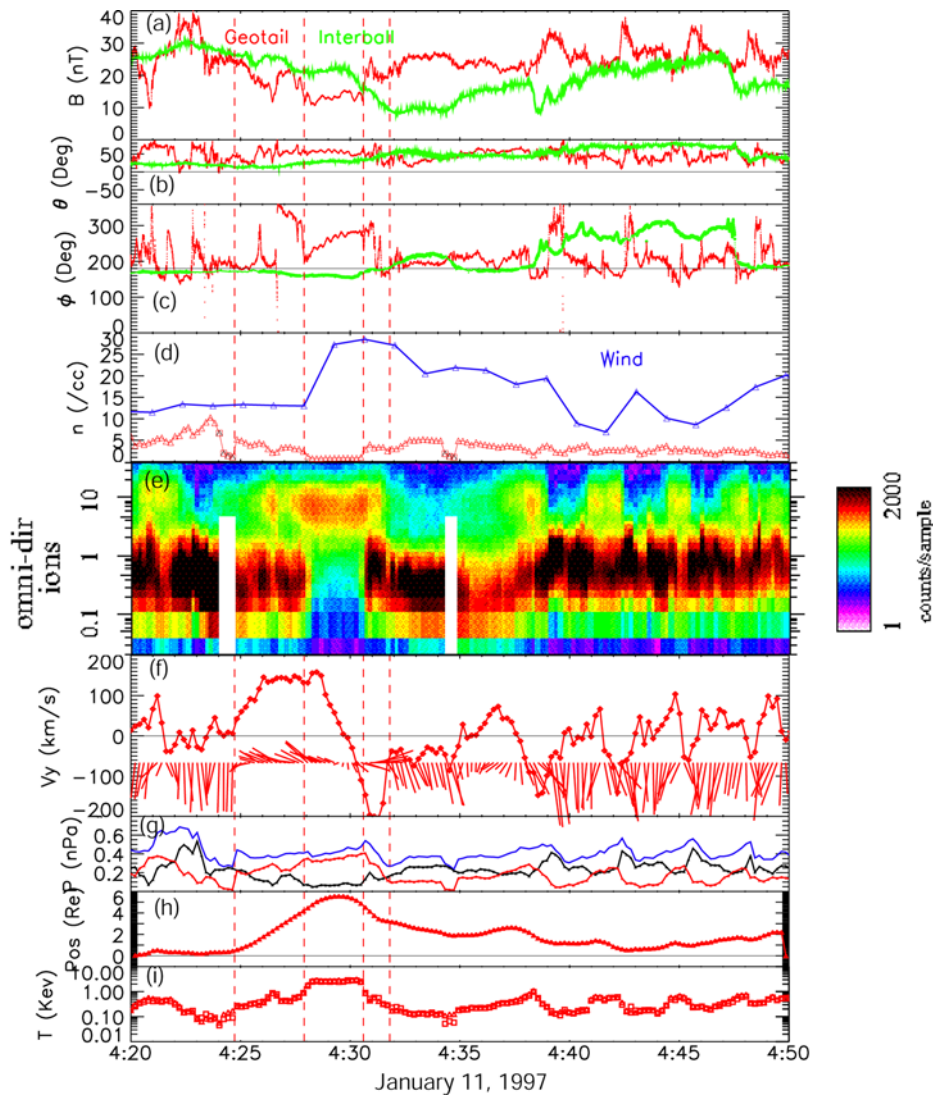


Figure 9. Interball and Geotail magnetic field strength, latitude angle θ and longitude angle ϕ are shown in Figures 9a–9c. Wind density and Geotail LEP density are shown in Figure 9d. A Geotail ion spectrogram is shown in Figure 9e. The V_y velocity, amplitude of motion, and ion temperature are again shown in Figures 9f, 9h, and 9i. Figure 9g shows magnetic field pressure (black), plasma pressure (red), and total pressure (blue).

boundary layer or magnetosheath, in fact the magnetosphere proper was briefly observed. We note also that the total pressure (the blue trace in Figure 9g) which is the sum of the field pressure (black trace) and plasma pressure (red trace) increases at 0421. (The low plasma pressures near 0424 result from the LEP instrument automatically switching to solar different mode due to high fluxes which results in 4 artificially low density data points indicated by squares in Figure 9d. The same thing happened at 0434.) Again the maxima in the position at 0429, indicating maximum penetration into the magnetosphere, corresponds to the temperature maxima characteristic of the magnetosphere proper. It is interesting to note the wave trains in the total pressure and V_y that are particularly prominent in the period 0438–0450. This behavior suggests a ringing of the magnetosphere following the incident pressure pulse.

[30] This interval provides another example of a pressure pulse causing large boundary motion as is illustrated in

Figure 6c. We suggest that a compression wave propagating faster than the pressure front in the magnetosheath arrived at Geotail in the boundary layer at 0425. The boundary moved outward into the lower-pressure magnetosheath, producing the duskward velocities at Geotail and the decreasing ϕ angle at Interball. A rarefaction follows the compression and either this lowering of the pressure or the arrival of the high-density magnetosheath plasma moves the boundary back inward. The demarcation line between high and low pressures in Figure 6c is drawn at an angle as in the earlier figures. The higher pressures are not sustained at subsequent times because the solar wind density begins decreasing after its initial increase.

6. Boundary Waves

[31] We investigate waves in the magnetopause/boundary layer by returning to the last 4 hours of 10 January where, as

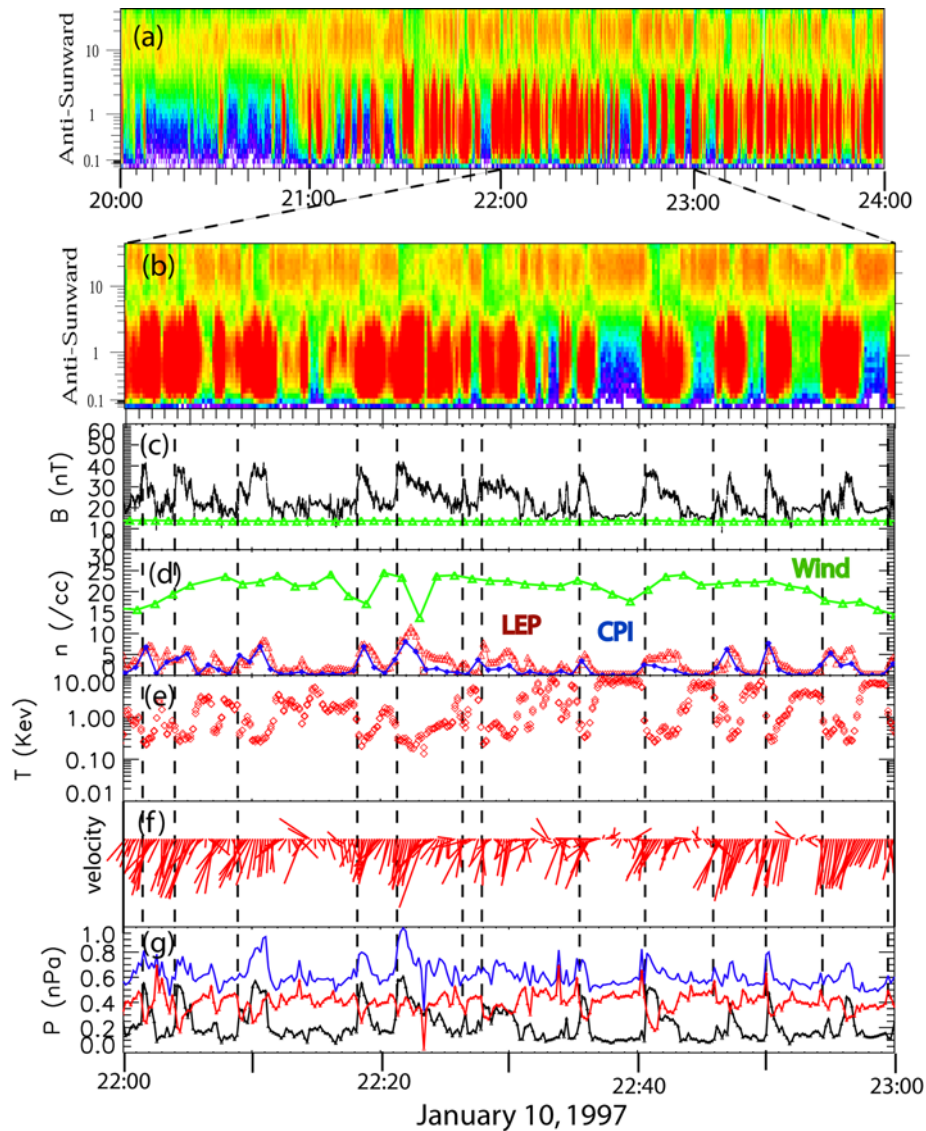


Figure 10. A 4 hour Geotail LEP ions spectrogram in Figure 10a is expanded to 1 hour in Figure 10b. Solar wind and Geotail magnetic field and density are shown in Figures 10c and 10d, respectively. Geotail temperature, velocity vectors and pressures are shown in Figures 10e–10g. Low Geotail densities relative to the solar wind along with low and variable velocities identify the region as boundary layer.

can be seen from Figure 3, Geotail was very near the expected magnetopause position and Interball was at least $2 R_E$ inside this boundary. Figure 10a shows a 4 hour Geotail LEP energy spectrogram for this interval. During the first hour, Geotail was mostly in the magnetosphere proper as predicted in Figure 2 and as is indicated by the intense plasma near 10 keV and the lack of lower-energy plasma. At later times the spectrogram shows more of a mixture of hot magnetosphere plasma and cool magnetosheath plasma as is characteristic of a boundary layer [e.g., *Fujimoto et al.*, 1998b]. Figures 10b–10g show an expanded view of the 2200–2300 hour. The spectrogram in Figure 10b shows some clear returns to the magnetosphere during the last 25 min as indicated by the lack of cool plasma, but more frequently there is a mixture of the two components. Figures 10c and 10d show magnetic field strength and density respectively with green indicating Wind measurements in the solar wind (advanced by 25 min) and red and blue the Geotail densities as measured by the Geotail

LEP in the hot plasma mode and Geotail CPI in the solar wind mode. Data from both these experiments are shown because the hot plasma mode might underestimate the density of the flowing magnetosheath plasmas and the solar wind mode might miss the low density, more isotropic, magnetosphere-like plasmas. The important point is that the measured densities are well below the interplanetary densities which should be roughly the same as the magnetosheath densities. This is in contrast to the measurements at 0020 and subsequent intervals on the next day (see Figure 4) where the Geotail densities are indeed greater than the solar wind densities. These low densities prior to 0020 and the accompanying variable velocities as shown in Figure 4 make it clear that Geotail remained in the boundary layer and did not enter the magnetosheath during the last 4 hours of 10 January. This conclusion agrees with that of *Laakso et al.* [1998] but is contrary to that of *Stenuit et al.* [2002], who assumed that during this interval Geotail was crossing a

boundary between the magnetosheath and the magnetosphere with no significant boundary layer.

[32] It is important to note in Figures 10c, 10d, and 10e that the density and field strength are highly correlated while the temperature is anticorrelated with them both. The variations are such that the high densities and low temperatures of the boundary layer tend to be in balance with the lower densities and higher temperatures of the magnetosphere as shown by the red trace in Figure 10g. The magnetic field pressure as shown by the black trace is usually lower than the plasma pressure indicating a plasma beta value greater than unity in the more interior magnetosphere-like region. Peaks in the field strength associated with the cooler plasma sometimes lead to total pressure peaks where beta is less than unity. These peaks, that tend to occur during transitions into the high-B, high-density regions and are marked by vertical dashed lines, are more abrupt than those in the reverse direction. This sawtooth type variation was also noted by *Scopke et al.* [1981]. Velocity vectors in the GSM XY plane are shown in Figure 10f using the same convention as earlier figures. V increases tend to accompany these B increases and the increased velocities invariably have an enhanced V_y component. Note that whereas in the previous section positive V_y indicated a duskward moving boundary that left the spacecraft in the hotter magnetosphere plasma, in Figure 10 the positive V_y accompanies entry into the higher-density, cooler boundary layer. This latter tendency can probably be explained by vortical motion [e.g., *Fairfield et al.*, 2000; *Otto and Fairfield*, 2000; *Stenuit et al.*, 2002] except the vortical explanation proposed by *Stenuit et al.* [2002] in their Figure 4 cannot be correct if the boundary is not the magnetopause.

[33] The Interball data taken simultaneously some 5 to 10 R_E tailward and 2 R_E interior to Geotail (see Figure 3) shows hot plasma similar to the magnetosphere plasma seen by Geotail during the 2000–2100 hour in Figure 10. This Interball data is not shown here but can be seen in Figure 7 of *Stenuit et al.* [2002]. Whereas *Stenuit et al.* argued for the absence of a boundary layer during this period, we believe Geotail was mostly within a boundary layer. It is more significant that Geotail never sees the magnetosheath during the interval of Figure 10. This 10 January interval is probably more similar to the interval studied by *Scopke et al.* [1981] which was in the dawn region near 0800 LT. These authors also observed a boundary layer but not the magnetosheath, and they argued that the KH instability was operative at the interface between the boundary layer and the magnetosphere. (These authors did not investigate interplanetary magnetic field conditions but a check of Imp 8 data shows a magnetic field mostly in the B_y direction which would tend to stabilize the magnetopause boundary.) *Stenuit et al.* [2002] argued that the magnetopause was not likely to be unstable during the 10 January interval, but perhaps it was the inner boundary that was unstable, which would help explain the lack of large amplitude waves leading to magnetopause crossings.

7. Ground Response to Magnetopause Motion

[34] Through electromagnetic coupling, the geomagnetic field at the Earth's surface responds to magnetopause motions, be they global motions (“breathing”) or waves

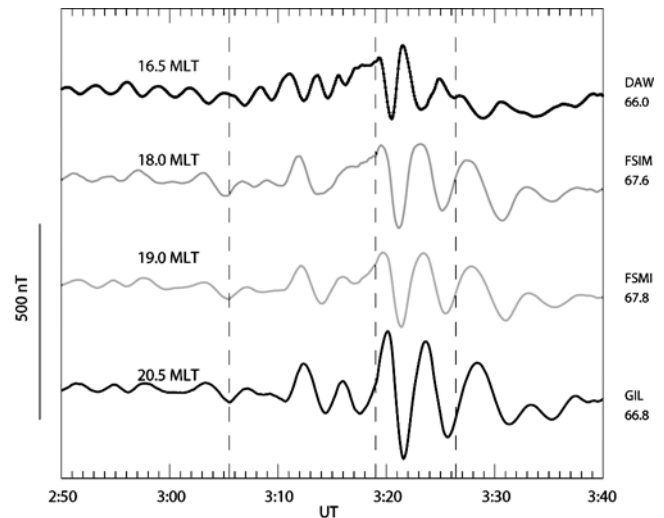


Figure 11. Data from the CANOPUS magnetometer chain showing stations at nearly the same latitude. Ongoing waves early in the interval are probably related to the Kelvin-Helmholtz instability of the magnetopause and the pulse of waves beginning at 0319 UT is caused by an interplanetary density change.

on this boundary, of whatever origin [e.g., *Farrugia et al.*, 1989; *Southwood and Kivelson*, 1990; *Freeman et al.*, 1990; *Samson*, 1991]. Such perturbations are evident in the data we have reviewed from five different magnetometer chains. Below we shall use a limited amount of data from two of these chains to illustrate the responses to different interplanetary triggers and any dawn-dusk asymmetries.

7.1. Response to Different External Triggers

[35] We first discuss observations from a chain of constant latitude stations spanning 4 hours of MLT on the duskside. The stations are DAW, FSIM, FSMI, and GIL from the CANOPUS array at corrected geomagnetic latitudes $67.1 \pm 0.8^\circ$. The H component traces for the time interval 0250–0340 UT are plotted in Figure 11 with the MLT at 0300 UT shown for each station. The vertical bar on the left indicates the scale.

[36] The following points may be made. (1) The effects of the pronounced pressure decrease at 0317 UT in Figures 1 and 2 are seen at all stations (the vertical dashed line denoting the onset occurs at 0319 since the effect takes some additional time to reach the flank). This response is MLT dependent; only one clear cycle is seen at station DAW, while evidence of “ringing” is seen at later local times, particularly at station GIL, where the signal amplitude has its maximum. This maximum suggests that GIL is on a resonating field line [*Farrugia et al.*, 1989; *Southwood and Kivelson*, 1990] which at 20.5 hours MLT will be a longer more tail-like field line compared with those from the same latitude at the earlier MLTs. The time lags between the peaks at the different stations confirm that the signal is propagating tailward. The wavelength appears to grow rapidly at earlier MLTs (as indicated by the greater separation of the initial peaks at FSIM compared with DAW) compared with later MLTs (where the separations are more nearly constant). The longer duration between peaks could

be due to a magnetosheath speed that is increasing faster at the earlier times, thus stretching the wavelength.

[37] (2) Prior to 0319 there are oscillations of period ~ 3 min (i.e., frequency ~ 5.6 mHz, in the Pc 5 range) at all stations but especially at DAW. These waves are probably the result of the ongoing magnetopause surface waves generated by the KH instability [Laakso *et al.*, 1998; Fairfield *et al.*, 2000; Farrugia *et al.*, 2000] during the strongly northward field interval. The energy in these micropulsations is coupled to the magnetopause motions by FACs [e.g., Samson, 1991; Kivelson and Chen, 1995; Farrugia *et al.*, 2001]. A phase shift is seen at DAW at 0305 and thereafter the background field increases and the waves have larger amplitude. These features are likely the result of the earlier pressure increase at 0303 in Figure 2.

7.2. Dawn-Dusk Asymmetries

[38] We next make a direct comparison between observations at two stations, one near dusk (GIL) and the other at dawn (SOR). These stations are at nearly identical corrected geomagnetic latitudes (67.0 ± 0.2 deg) and at 0300 UT they are at 2030 MLT (GIL) and at 0554 MLT (SOR). Figure 12 shows the same interval as in Figure 11, with GIL as the thick trace. Both the ongoing waves and those resulting from the pressure change are seen at both stations. The frequencies are similar at the two stations although the waves are somewhat more regular at SOR, particularly early in the interval. A difference between the two stations is that the amplitudes of the pressure-associated waves are larger at dusk by about a factor of 2.

8. Summary and Discussion

[39] Using data from 10–11 January 1997, we have utilized a fortuitous two spacecraft configuration near the dusk magnetopause to study two different types of perturbations of this boundary region. The effects of several large interplanetary density discontinuities have been successively measured by these two spacecraft along with Goes 9. The primary result confirms theoretical expectations [Kaufmann and Konradi, 1969; Sibeck, 1990] of how a pressure wave produced near the subsolar point can travel tailward in the magnetosphere/boundary layer ahead of the discontinuity front in the magnetosheath. A positive pressure change creates a positive pressure wave that will cause the magnetopause to bulge out as is illustrated by the red magnetopause in Figure 13, a figure which is similar to the sketch in Figure 16 of

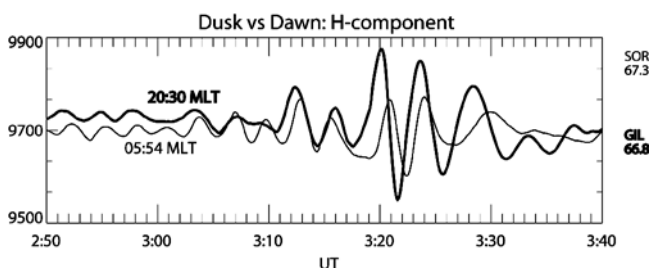


Figure 12. Data from ground magnetometer stations of nearly the same latitudes near dawn and dusk. The similarity of the waves indicates their global nature.

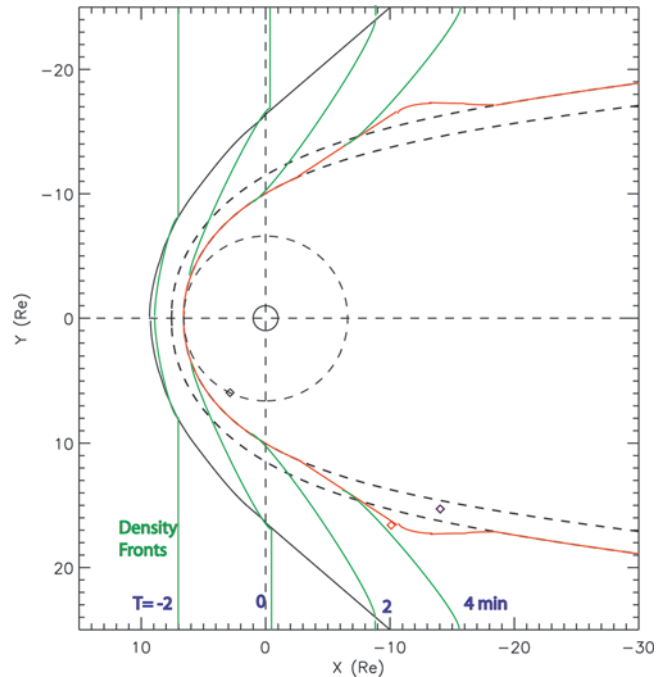


Figure 13. The red trace illustrates a likely magnetopause position during the transition between two equilibrium positions (dashed lines) corresponding to two sides of a discontinuity front where the pressure increases. Green lines indicate typical positions of the discontinuity front at times relative to its arrival at the subsolar magnetopause. A fast mode wave in the boundary layer propagates ahead of the pressure front in the magnetosheath causing the magnetopause to bulge out in the region ahead of the pressure increase. Magnetosheath pressure fronts make an acute angle with the magnetopause since plasma near this boundary has been delayed due to passage near the subsolar stagnation region.

Kaufmann and Konradi [1969]. This red trace joins the initial and final equilibrium magnetopause positions calculated from the Shue *et al.* [1998] model as represented by dashed lines. A spacecraft in the magnetosheath may briefly encounter the magnetosphere as the bulge moves past (or a spacecraft in the boundary layer may briefly encounter the bulging magnetosphere proper as in Figure 9 near 0430). A spacecraft in the magnetosphere may cross into the magnetosheath as an indentation following the bulge moves past (0121 20s in Figure 5 and Figure 6a). Both effects on the leading and trailing sides of the bulge occur before the magnetosheath density front arrives. In a similar manner, a density decrease can launch a rarefaction wave that causes an indentation ahead of the magnetosheath front. In this case, a spacecraft in the magnetosphere might experience an early brief period in the magnetosheath or a magnetosheath spacecraft outside the new more distant equilibrium magnetopause position might experience a brief period within the magnetosphere (Geotail near 0209 and 0223 in Figure 7 and Figure 6b; Geotail 0324 in Figure 8).

[40] It was also concluded that the density front in the magnetosheath forms an acute angle with the magnetopause as is shown in Figures 6 and 13. This is undoubtedly due to

plasma nearer the magnetopause having passed nearer the stagnation point where it is delayed, thus skewing the front in the magnetosheath. This slower magnetosheath velocity also makes it more likely that the pressure pulse in the boundary layer will exceed that in the magnetosheath.

[41] During the last four hours on 10 January the fast mode wave speed in the boundary layer at Geotail is close to the solar wind velocity with the sonic and Alfvén velocities being roughly equivalent. During magnetosphere intervals detected at this location, the fast mode speed is two to three times that of the boundary layer due primarily to high sonic velocities resulting from the higher temperatures. After the magnetosheath intervals on 11 January, the fast mode speeds in the boundary layer tend to be somewhat lower than those several hours earlier, with the Alfvén speed greater than the sonic speed due to lower temperatures. These lower fast mode wave speeds at later times are probably due to Geotail's location further down tail. Fast mode speed in the boundary layer should be largest near the subsolar point where the magnetic field and temperatures are largest and it should decrease with distance from the subsolar point due to the decreasing temperature and magnetic field strength and perhaps an increasing density.

[42] In studying the pressure front in the magnetosheath, evidence was presented showing how the higher-density region, which contains greater thermal pressure than the lower-density region after passing through the bow shock, expands into the lower-density region. This expansion produces an interval adjacent to the discontinuity with density, temperature, and magnetic field lower than that in the high-density region. If the high-pressure region follows the lower-pressure region, the higher-pressure plasma expands in the downstream direction and thus increases the velocity. If the high pressure precedes the low pressure, the expansion in the upstream direction decreases the magnetosheath velocity.

[43] During the 10 January interval of Figure 10, we argued that Geotail spent most of its time observing relatively high, several per cubic centimeter densities of the boundary layer. The periodic motions of the magnetosphere/boundary layer interface suggest that the KH instability was operating and might be responsible for moving magnetosheath particles into the magnetosphere [Otto and Fairfield, 2000; Nykyri and Otto, 2001]. In contrast, Stenuit *et al.* [2002] assumed that the dense particle region was the magnetosheath and there was no particle entry to a boundary layer which supported their argument that the KH instability was not instrumental in transporting particles into the magnetosphere despite the persistent northward IMF. Another part of these authors argument against the importance of the KH instability in creating a boundary layer was the energy spectrogram of the interval from 0425 to 0435 presented in their Figure 5, an interval included in our Figure 9. They noted the lack of flow in the X direction and the short duration of intervals of overlapping hot magnetosphere particles and cool magnetosheath-like plasmas that appeared adjacent to the hot plasma boundaries at 0428 and 0432 30 s. On the basis of these short 1 and 2 min intervals, they concluded that there was only a very narrow region of plasma mixing, deeming it "unlikely" that Geotail penetrated deep into the magnetosphere. Using the V_y velocities in our Figure 9f, it is clear that Geotail did in

fact penetrate a substantial distance into the magnetosphere. Using the observed V_y duskward velocities of 160 km/s for 2 min and dawnward velocities of 190 km/s for 1 min, one obtains thick mixed plasma regions of 3 and 1.8 R_E respectively. The more extended spectrogram in Figure 9e also shows subsequent intervals of mixed plasma. This reevaluation casts further doubt on their conclusion that the KH instability had not produced a thick mixing region despite the fact that the IMF had been northward for some 7 hours. We conclude that the 10–11 January 1997 interval supports the idea that the KH instability is operative during periods of very northward IMF and it may be an important mechanism for transporting magnetosheath particles into the magnetosphere. How often this process occurs remains to be determined.

[44] **Acknowledgments.** We gratefully acknowledge A. Lazarus and J. Kasper of MIT for providing the SWE plasma data and the Wind MFI team for the magnetometer data. We are also indebted to J-A. Sauvaud for the Interball electron data, Y. Yermolaev for the CORALL Interball ion data, and S. Romanov for the MIF Interball magnetic field data. H. Singer was responsible for the GOES 9 magnetic field data and L. Frank the Geotail CPI data. We thank A. Viljanen and the German-Finnish-Norwegian-Polish IMAGE project team led by the Technical University of Braunschweig for the Scandinavian magnetometer data. The Canadian Space Agency constructed, maintains, and operates the CANOPUS instrument array, and we thank T. Hughes for providing this magnetometer data. The CBI data are provided by the CPMN group, and we thank the Solar-Terrestrial Environment Laboratory, Nagoya University, for the construction of the 210MM database. The work of DHF and CJF is supported by the National Aeronautics and Space Administration under a grant issued through the Sun-Earth Connection Guest Investigator program.

[45] Lou-Chuang Lee thanks William Lotko for the assistance in evaluating this paper.

References

- Aubry, M. P., M. G. Kivelson, and C. T. Russell, Motion and structure of the magnetopause, *J. Geophys. Res.*, 76, 1673, 1971.
- Burlaga, L., et al., A magnetic cloud containing prominence material: January 1997, *J. Geophys. Res.*, 103, 277, 1998.
- Chapman, S., and J. Bartels, *Geomagnetism*, Oxford Univ. Press, New York, 1940.
- Chen, S.-H., and M. G. Kivelson, On nonsinusoidal waves at the Earth's magnetopause, *Geophys. Res. Lett.*, 20, 2699, 1993.
- Chen, S.-H., M. G. Kivelson, J. T. Gosling, R. J. Walker, and A. J. Lazarus, Anomalous aspects of magnetosheath flow and of the shape and oscillations of the magnetopause during an interval of strongly northward interplanetary magnetic field, *J. Geophys. Res.*, 98, 5727, 1993.
- Fairfield, D. H., W. Baumjohann, G. Paschmann, H. Luhr, and D. G. Sibeck, Upstream pressure variations associated with the bow shock and their effects on the magnetosphere, *J. Geophys. Res.*, 95, 3773, 1990.
- Fairfield, D. H., A. Otto, T. Mukai, S. Kokubun, R. P. Lepping, J. T. Steinberg, A. J. Lazarus, and T. Yamamoto, Geotail observations of the Kelvin-Helmholtz instability at the equatorial magnetotail boundary for parallel northward fields, *J. Geophys. Res.*, 105, 21,159, 2000.
- Farrugia, C. J., M. P. Freeman, S. W. H. Cowley, D. J. Southwood, M. Lockwood, and A. Etemadi, Pressure-driven magnetopause motions and attendant response on the ground, *Planet. Space Sci.*, 37, 589, 1989.
- Farrugia, C. J., et al., Geoeffectiveness of three WIND magnetic clouds: A comparative study, *J. Geophys. Res.*, 103, 17,261, 1998.
- Farrugia, C. J., et al., Coordinated Wind, Interball/tail, and ground observations of Kelvin-Helmholtz waves at the near-tail, equatorial magnetopause at dusk: January 11, 1997, *J. Geophys. Res.*, 105, 7639, 2000.
- Farrugia, C. J., F. T. Gratton, and R. B. Torbert, The role of viscous-type processes in solar wind-magnetosphere interactions, *Space Sci Rev.*, 95, 443, 2001.
- Freeman, M. P., and C. J. Farrugia, Magnetopause motions in a Newton-Busemann approach, in *Polar Cap Boundary Phenomena*, p. 15, edited by J. Moen et al., Kluwer Acad., Norwell, Mass., 1998.
- Freeman, M. P., C. J. Farrugia, S. W. H. Cowley, S. J. Southwood, M. Lockwood, and A. Etemadi, The response of the magnetosphere-ionosphere system to solar wind dynamic pressure variations, in *Physics of Magnetic Flux Ropes*, *Geophys. Monogr. Ser.*, vol. 58, edited by C. T. Russell, E. R. Priest, and L. C. Lee, p. 611, AGU, Washington, D. C., 1990.

- Fujimoto, M., and T. Terasawa, Anomalous ion mixing within an MHD scale Kelvin-Helmholtz vortex: 2. Effects of inhomogeneity, *J. Geophys. Res.*, *100*, 12,025, 1995.
- Fujimoto, M., A. Nishida, T. Mukai, Y. Saito, T. Yamamoto, and S. Kokubun, Plasma entry from the flanks of the near-Earth magnetotail: Geotail observations in the dawnside LLBL and the plasma sheet, *J. Geomagn. Geoelectr.*, *48*, 711, 1996.
- Fujimoto, M., T. Mukai, H. Kawano, M. Nakamura, A. Nishida, Y. Saito, T. Yamamoto, and S. Kokubun, Structure of the low-latitude boundary layer: A case study with Geotail data, *J. Geophys. Res.*, *103*, 2297, 1998a.
- Fujimoto, M., T. Terasawa, T. Mukai, Y. Saito, T. Yamamoto, and S. Kokubun, Plasma entry from the flanks of the near-Earth magnetotail: Geotail observations, *J. Geophys. Res.*, *103*, 4391, 1998b.
- Kaufmann, R. L., and A. Konradi, Explorer 12 magnetopause observations: Large-scale nonuniform motion, *J. Geophys. Res.*, *74*, 3609, 1969.
- Kivelson, M. G., and S.-H. Chen, The Magnetopause: Surface waves and instabilities and their possible dynamical consequences, in *Physics of the Magnetopause*, *Geophys. Monogr. Ser.*, vol. 90, edited by P. Song, B. U. O. Sonnerup, and M. F. Thomsen, pp. 257–268, AGU, Washington, D. C., 1995.
- Kokubun, S., H. Kawano, T. Mukai, Y. Saito, K. Tsuruda, T. Yamamoto, and G. Rostoker, Surface waves on the dawn magnetopause: Connection with Ground PC 5 pulsations, *Adv. Space Res.*, *25*(7/8), 1493, 2000.
- Laakso, H., et al., Field-line resonances triggered by a northward IMF turning, *Geophys. Res. Lett.*, *25*, 2991, 1998.
- Larson, D. E., R. P. Lin, and J. Steinberg, Extremely cold electrons in the January 1997 magnetic cloud, *Geophys. Res. Lett.*, *27*, 157, 2000.
- Le, G., C. T. Russell, and J. T. Gosling, Structure of the magnetopause for low Mach number and strongly northward interplanetary magnetic field, *J. Geophys. Res.*, *99*, 23,723, 1994.
- Le, G., C. T. Russell, J. T. Gosling, and M. F. Thomsen, ISEE observations of low-latitude boundary layer for northward interplanetary magnetic field: Implications for cusp reconnection, *J. Geophys. Res.*, *101*, 27,239, 1996.
- Ledley, B. G., Magnetopause attitudes during Ogo 5 Crossings, *J. Geophys. Res.*, *76*, 6736, 1971.
- Lepping, R. P., et al., The Wind magnetic field investigation, in *The Global Geospace Mission*, edited by C. T. Russell, p. 207, Kluwer Acad., Norwell, Mass., 1995.
- Lotko, W., and B. U. O. Sonnerup, The low-latitude boundary layer on closed field lines, in *Physics of the Magnetopause*, *Geophys. Monogr. Ser.*, vol. 90, edited by P. Song et al., p. 371, AGU, Washington, D. C., 1995.
- Nishida, A., *Geomagnetic Diagnosis of the Magnetosphere*, Springer-Verlag, New York, 1978.
- Nykyri, K., and A. Otto, Plasma transport at the magnetospheric boundary due to reconnection in Kelvin-Helmholtz vortices, *Geophys. Res. Lett.*, *28*, 3565, 2001.
- Ogilvie, K. W., et al., SWE, a comprehensive plasma instrument for the Wind spacecraft, in *The Global Geospace Mission*, edited by C. T. Russell, p. 55, Kluwer Acad., Norwell, Mass., 1995.
- Otto, A., and D. H. Fairfield, Kelvin-Helmholtz instability at the magnetotail boundary: MHD simulation and comparison with Geotail observations, *J. Geophys. Res.*, *105*, 21,175, 2000.
- Paschmann, G., W. Baumjohann, N. Sckopke, and T.-D. Phan, Structure of the dayside magnetopause for low magnetic shear, *J. Geophys. Res.*, *98*, 13,409, 1993.
- Phan, T. D., et al., Low-latitude dusk flank magnetosheath, magnetopause, and boundary layer for low magnetic shear: Wind observations, *J. Geophys. Res.*, *102*, 19,883, 1997.
- Russell, C. T., M. Ginskey, S. Petrinc, and G. Le, The effect of solar wind dynamic pressure changes on low to mid-latitude magnetic records, *Geophys. Res. Lett.*, *19*, 1227, 1992.
- Samson, J. C., Geomagnetic pulsations and plasma waves in the Earth's magnetosphere, in *Geomagnetism*, vol. 4., pp. 481, Academic, San Diego, Calif., 1991.
- Sandholt, P. E., C. J. Farrugia, S. W. H. Cowley, and W. F. Denig, Capture of magnetosheath plasma by the magnetosphere during northward IMF, *Geophys. Res. Lett.*, *26*, 2833, 1999.
- Sckopke, N., G. Paschmann, G. Haerendel, B. U. O. Sonnerup, S. J. Bame, T. G. Forbes, E. W. Hones Jr., and C. T. Russell, Structure of the low-latitude boundary layer, *J. Geophys. Res.*, *86*, 2099, 1981.
- Shue, J.-H., et al., Magnetopause location under extreme solar wind conditions, *J. Geophys. Res.*, *103*, 17,691, 1998.
- Sibeck, D. G., A model for the transient magnetospheric response to sudden solar wind dynamic pressure variations, *J. Geophys. Res.*, *95*, 3755, 1990.
- Song, P., and C. T. Russell, Model of the formation of the low-latitude boundary layer for strongly northward interplanetary magnetic field, *J. Geophys. Res.*, *97*, 1411, 1992.
- Southwood, D. J., and M. G. Kivelson, The magnetohydrodynamic response of the magnetospheric cavity to changes in solar wind pressure, *J. Geophys. Res.*, *95*, 2301, 1990.
- Stenuit, H., et al., Multispacecraft study on the dynamics of the dusk-flank magnetosphere under northward IMF: 10–11 January 1997, *J. Geophys. Res.*, *107*(A10), 1333, doi:10.1029/2002JA009246, 2002.
- Tamao, T., A hydromagnetic interpretation of geomagnetic SSC*, *Rep. Ionos. Space Res. Jpn.*, *18*, 16, 1964.
- Terasawa, T., et al., Solar wind control of density and temperature in the near-Earth plasma sheet: Wind-Geotail collaboration, *Geophys. Res. Lett.*, *24*, 935, 1997.
- Völk, H. J., and R.-D. Auer, Motions of the bow shock induced by interplanetary disturbances, *J. Geophys. Res.*, *79*, 40, 1974.
- Wu, B. H., M. E. Mandt, L. C. Lee, and J. K. Chao, Magnetospheric response to solar wind dynamic pressure variations: Interaction of interplanetary tangential discontinuities with the bow shock, *J. Geophys. Res.*, *98*, 21,297, 1993.

D. H. Fairfield, Laboratory for Extraterrestrial Physics, NASA Goddard Space Flight Center, Mail Code 695, Greenbelt, MD 20771, USA. (donald.h.fairfield@nasa.gov)

C. J. Farrugia, Space Science Center, University of New Hampshire, 39 College Road, Durham, NH 03824, USA. (charlie.farrugia@unh.edu)

A. Federov, Centre d'Etude Spatiale des Rayonnements, 9 av. du Colonel-Roche, B.P. 4346, 31028 Toulouse Cedex 4, France. (andrei.federov@cesr.fr)

T. Mukai, Institute of Space and Astronomical Science, 3-1-1 Yoshinodai, Sagami-hara, Kanagawa 229-8510, Japan. (mukai@stp.isas.ac.jp)

T. Nagai, Earth and Planetary Sciences, Tokyo Institute of Technology, Tokyo 152-8551, Japan. (nagai@geo.titech.ac.jp)